Journal of Hazardous Materials 185 (2011) 322–328

Contents lists available at ScienceDirect

Journal of Hazardous Materials

journal homepage: www.elsevier.com/locate/jhazmat

Removal of metals from aqueous solution and sea water by functionalized graphite nanoplatelets based electrodes

Ashish Kumar Mishra, S. Ramaprabhu*

Alternative Energy and Nanotechnology Laboratory (AENL), Nano Functional Materials Technology Centre (NFMTC), Department of Physics, Indian Institute of Technology Madras, Chennai 600036, India

ARTICLE INFO

Article history:
Received 9 July 2010
Received in revised form 4 September 2010
Accepted 6 September 2010
Available online 17 September 2010

Keywords:
Functionalized graphite nanoplatelets
Water purification
Sodium removal
Arsenic removal
Supercapacitor

ABSTRACT

In the present wok, we have demonstrated the simultaneous removal of sodium and arsenic (pentavalent and trivalent) from aqueous solution using functionalized graphite nanoplatelets (*f*-GNP) based electrodes. In addition, these electrodes based water filter was used for multiple metals removal from sea water. Graphite nanoplatelets (GNP) were prepared by acid intercalation and thermal exfoliation. Functionalization of GNP was done by further acid treatment. Material was characterized by different characterization techniques. Performance of supercapacitor based water filter was analyzed for the removal of high concentration of arsenic (trivalent and pentavalent) and sodium as well as for desalination of sea water, using cyclic voltametry (CV) and inductive coupled plasma-optical emission spectroscopy (ICP-OES) techniques. Adsorption isotherms and kinetic characteristics were studied for the simultaneous removal of sodium and arsenic (both trivalent and pentavalent). Maximum adsorption capacities of 27, 29 and 32 mg/g for arsenate, arsenite and sodium were achieved in addition to good removal efficiency for sodium, magnesium, calcium and potassium from sea water.

1. Introduction

Water has great copiousness on the Earth, and of that about 97% is sea water. Fresh water which can be utilized by man is only 1% of sea water. Sea water contains about 3.5% by weight of salt. High percentage of salinity in sea water is the main impediment for the utilization of sea water for domestic purposes. Salinity of sea water is due to the presence of metals like sodium, magnesium, calcium, potassium, etc. Sodium and magnesium have the maximum concentrations in sea water among all metals. Currently implemented technologies for obtaining sea water into fresh water, such as multi-stage flash, multiple effect distillation, vapor compression distillation, reverse osmosis and electric dialysis have problems of difficult maintenance such as complex pretreatment of sea water, high energy consumption and some use membranes operated at high pressures. The primary argument against using sea water as a water source has been the high cost of sea water desalination. New water techniques consume energy, and innovative renewable energy techniques using biofuels and biodiesel consume an incredible amount of water [1–5]. Therefore there is a need of cost effective technology which can provide alternative solutions to these problems.

Ground water is the other source for human society. Arsenic in groundwater has become a serious problem to humanity because of its toxicity. Throughout the world, arsenic is creating potentially serious environmental problems for humans and other living organisms. Arsenic occurs with valence states of −3, 0, +3 (arsenite, As [III]) and +5 (arsenate, As [V]). The valence states −3 and 0 occur rarely. Chiefly arsenic is available in water as arsenite [$(AsO_3)^{3-}$] and arsenate [$(AsO_4)^{3-}$]. Exposure to inorganic arsenic can cause various health effects, such as irritation of the stomach and intestines, decreased production of red and white blood cells, skin changes and lung irritation. Different treatment techniques like coagulation, reverse osmosis, ion exchange, flotation and adsorption on metal oxides (iron oxides, activated alumina), mixed metal oxides and resin were reported mainly for pentavalent arsenic removal [6–12]. Activated carbon based sorbents have been tested for arsenic removal with very low adsorbent capacity [13,14]. Therefore there is a need for a new material and technology, which can provide solutions for the removal of both types of inorganic arsenic species.

The electrochemical methods find several applications, such as metal ion removal and recovery, electro-dialysis, electrodeionisation, and especially, destruction of toxic and non-biodegradable organics. The electrochemical technologies have attracted a great deal of attention because of their versatility, which makes the treatment of liquids, gases and solids possible and environmental compatibility. Copper ions were removed with high efficiency

* Corresponding author. Tel.: +91 44 22574862; fax: +91 44 22570509.
E-mail address: ramp@iitm.ac.in (S. Ramaprabhu).

0304-3894/$ – see front matter © 2010 Elsevier B.V. All rights reserved.
doi:10.1016/j.jhazmat.2010.09.037

from a dilute industrial effluent in an electrochemical reactor with plate electrode [15]. A combination of electrochemical and biological processes was carried out to recover copper, nickel and chromium from sludge of publicly owned treatment works and industrial effluents [16].

Recently, we demonstrated the use of Fe_3O_4-MWNTs based supercapacitor for arsenic removal and desalination of sea water [17]. Since MWNTs are costly hence there is need of cost effective utilization of this technique for large scale. In this context we have prepared functionalized graphite nanoplatelets by very simple and cost effective technique. In the present work, we have demonstrated for the first time the utilization of graphite nanoplatelets (GNP) for simultaneous removal of sodium and both types of inorganic arsenic species (trivalent and pentavalent) from aqueous solution and simultaneous removal of multiple metals like sodium (Na), magnesium (Mg), calcium (Ca) and potassium (K) from sea water. In addition, isotherm and kinetic adsorption behaviors of functionalized graphite nanoplatelets for sodium and arsenic were examined.

2. Experimental

2.1. Preparation of functionalized graphite nanoplatelets

Graphite was vigorously stirred with conc. HNO_3 and conc. H_2SO_4 in 1:3 ratios for three days. Vigorous stirring of graphite under strong acidic medium may cause the formation of acid intercalated graphite. This intercalated graphite further thermally exfoliated at 1000 °C. This thermal shock may lead to the destacking of the graphite plates and hence formation of GNP [18]. This GNP was further treated with conc. HNO_3, which introduces hydrophilic functional groups (–COOH, –C=O, and –OH) at the surface of GNP. These functionalized graphite nanoplatelets (*f*-GNP) were further washed several times with water to achieve pH = 7 followed by drying [19]. Hydrophilic nature of *f*-GNP provides better contact between water and electrode.

2.2. Preparation of electrode and electrolyte

The carbon fabric was supplied by SGL, Germany. Electrodes were prepared using dispersed solution of *f*-GNP in ethanol and few drops of nafion. Gel solution was coated on carbon fabric using spray coating technique. Further these *f*-GNP coated carbon fabrics were hot pressed at 50 °C under 1 ton force for 15 min to provide good mechanical strength to the electrodes. Glassy carbon electrode (GCE) was modified with *f*-GNP for cyclic voltametry (CV) analysis. Functionalized graphite nanoplatelets (5 mg) were sonicated in 0.2 ml of ethanol for 15 min followed by the addition of 5 μl of nafion in each solution. This gel solution was again sonicated for 10 min and 2 μl of the gel solution was deposited on GC electrode and dried at room temperature.

Sodium arsenate and sodium arsenite (both from Across Organics) were selected as the solutes for two types of arsenic ions. Two different arsenic ions containing water and sea water were taken as electrolytes for supercapacitor based water filter. Sea water sample was collected from Bay of Bengal shores at Chennai, India. Sodium arsenate and sodium arsenite containing water having initial concentration 300 ppm of arsenic were used for kinetic studies. Isotherm studies were performed with different initial concentrations (50–300 ppm) of arsenic with both types of arsenic ions. Volumes of 65 ml for sodium arsenate and sodium arsenite containing water were used to study isotherm and kinetic characteristics of *f*-GNP for simultaneous removal of arsenic and sodium. To study the cyclic repeatability of electrodes, 100 ml of arsenic containing water (both arsenate and arsenite) was used. Ability of this supercapacitor based water filter for the simultaneous removal of multiple metals from sea water was also tested with 100 ml of sea water.

2.3. Fabrication of the apparatus

Cylindrical perspex of length 2 cm, width 0.5 cm and diameter 4 cm was used for water collection between the electrodes. At both the ends, carbon fabric supported *f*-GNP based electrodes were fixed. Stainless steel plates were used as current collector and graphite plates were used to provide conducting support to the electrodes. Schematic for the designing of set up used for the present study is shown in Fig. 1. DC regulated power supply was used to give 1 V across the electrodes. In treatment of sea water as well as for arsenic containing water, the amount of *f*-GNP was 100 mg at each electrode.

2.4. Characterization

Surface morphology of *f*-GNP was characterized by Quanta 3D FEG scanning electron microscope and structural study by JEOL 3010 High resolution transmission electron microscope. Raman analysis was performed using HORIBA JOBIN YVON HR800UV Confocal Raman Spectrometer, while Fourier transform infrared spectroscopy (FTIR) study was performed using PERKIN ELMER Spectrum One FT-IR spectrometer. In order to investigate the electrochemical activity of *f*-GNP, CV was performed using CH instrument (CHI608C). To confirm the removal of sodium and arsenic, Inductive coupled plasma optical emission spectroscopy (ICP-OES) analysis was carried out using PERKIN-ELMER OPTIMA 5300DV ICP-OES instrument.

3. Results and discussion

3.1. Morphological and structural study

TEM (Fig. 2a) and SEM (Fig. 2b) images of *f*-GNP reveal its morphological structure. TEM and SEM images clearly suggest the induced disorderness in graphite structure. X-ray diffractogram of pure graphite and *f*-GNP is shown in Fig. 2c. X-ray pattern clearly shows less number of counts for *f*-GNP compared to pure graphite. This may be attributed to the destacking of ordered graphitic structure [20].

3.2. Fourier transform infrared and Raman spectrograms analysis

FTIR spectrum analysis of pure graphite and *f*-GNP is shown in Fig. 3a. In case of pure graphite, the band corresponding to hydroxyl group (–OH, 3428 cm^{-1}) is present significantly with very small ratio of anti-symmetric and symmetric $=CH_2$ vibrations (2920 and 2848 cm^{-1}) at the surface of pure graphite. In the case of pure graphite, >C = C (1635 and 1581 cm^{-1}) and bending of =CH– (1371 cm^{-1}) also present along with the above mentioned –OH and $-CH_2$ vibration bands. In case of *f*-GNP, the intensities of these peaks increase along with a presence of new peak at 1459 cm^{-1}, corresponding to the carboxylic (–COOH) group [21]. In addition, >C=C (1638 cm^{-1}), bending of =CH– (1376 cm^{-1}), >C=O (1052 cm^{-1}), the band corresponding to hydroxyl group (–OH, 3448 cm^{-1}), anti-symmetric and symmetric $=CH_2$ vibrations (2920 and 2839 cm^{-1}) are also present. FTIR study confirms the defective sites at the surface of *f*-GNP and the presence of $=CH_2$, >C=O, –COOH and –OH functional groups on the surface of *f*-GNP, which leads to the hydrophilic nature of *f*-GNP [22]. These functional groups are responsible to provide better contact between water and electrodes.

Raman spectrum analysis of pure graphite and *f*-GNP is shown in Fig. 3b. Figure shows the two peaks D-band (1346 cm^{-1}) and

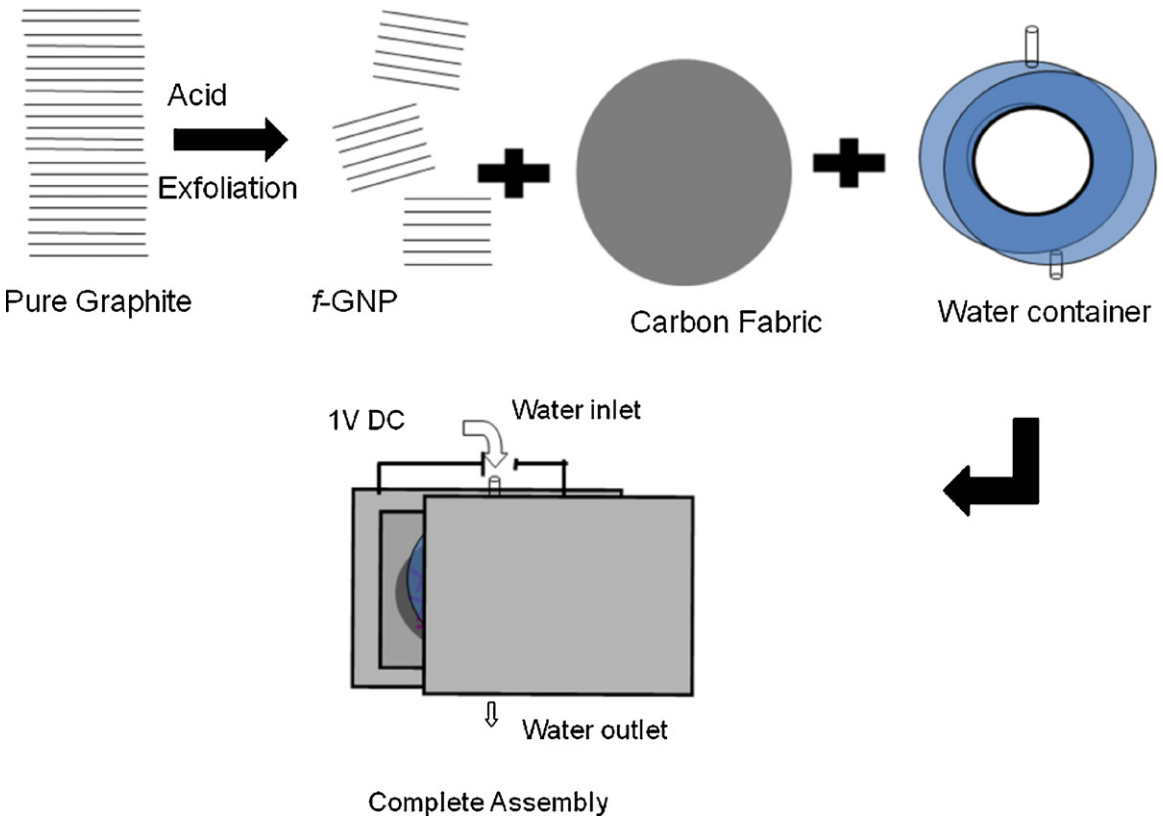

Fig. 1. Schematic design of functionalized graphite nanoplatelets based supercapacitor.

G-band (1575 cm^{-1}) for pure graphite. Very low intensity of D-band compared to the G-band attributes to the high degree of order present in pure graphite. The ratio of the intensity of D-band to G-band, i.e. I_D/I_G was found to be 0.602. The positions of D-band and G-band peaks change to the lower Raman shift value (1342 and 1571 cm^{-1}, respectively) and value of I_D/I_G was found to be 0.674 for *f*-GNP, which suggests the increase in defects or disorderness in graphitic structure. Some degree of disorder could be due to line defects and functional groups attached to the surface of *f*-GNP [23]. These functional groups at the surface of GNP provide hydrophilic nature to *f*-GNP [21].

3.3. Electrochemical analysis

In addition, CV was performed to check the electrochemical activity of *f*-GNP towards arsenate, arsenite and sodium ions. In CV analysis, Ag/AgCl and Pt wire electrodes were taken as reference and counter electrodes, respectively, *f*-GNP modified glassy carbon electrode was taken as working electrode. CV analysis was performed with aqueous solutions of sodium arsenate and sodium arsenite and sea water as electrolytes with a constant scan rate of 10 mV/s. Fig. 4 shows the cyclic voltamograms for all the electrolytes. The almost rectangular shapes of cyclic voltamograms obtained with each electrolyte suggest the formation of double layer at electrode and electrolyte interface. Cathodic peaks (arsenate, arsenite and sea water) correspondingly, may stand for reduction from arsenate to arsenite or from arsenite to elemental arsenic [17,24]. A slight shift was observed in sea water, which may be attributed to the presence of other metallic impurities (Mg, Ca, K, etc.) present in sea water. These cathodic peaks of voltamograms (Fig. 4) suggest the redox reactions and double layer formation of arsenic in arsenic based water and sea water. Absence of any peak corresponding to sodium suggests the double layer formation of sodium ions at the electrode–electrolyte interface.

Under the influence of the electrostatic force, these ions are attracted towards the opposite charged electrodes of supercapacitor. When these ions move to the surface of electrodes, they get adsorbed at the surface due to large number of anchoring sites at the surface of *f*-GNP. Functional groups may create the intermediate bonding between water molecules and *f*-GNP which provide better contact between electrodes and electrolyte. This leads to the high capacitance of supercapacitor due to the small separation between electrode and electrolytic ions (metal impurity). This suggests more number of ions at the electrode interface and hence more metal removal in single treatment. After continuous cycles of treatment, due to metal adsorption number of available anchoring sites reduces. In order to regain the anchoring sites of the electrode material, reverse voltage was applied with an optimized fast flow of water. Under the influence of reverse voltage, the adsorbed ions at the electrodes get detached and were harmlessly treated in the end. This helps the electrodes to regain their anchoring sites for further use.

3.4. Adsorption isotherm studies

The quantity of the metallic impurities that could be adsorbed at *f*-GNP surface is a function of concentration, which could be explained by adsorption isotherms. In the present study, Langmuir and Freundlich isotherms were tested with the simultaneous removal of sodium and arsenic [25,26]. Sodium arsenate and sodium arsenite containing aqueous solutions with the initial arsenic concentrations varying from 50 to 300 ppm were used for above purpose. Langmuir isotherm assumes that the single adsorbate binds to a single site on the adsorbent and that all surface

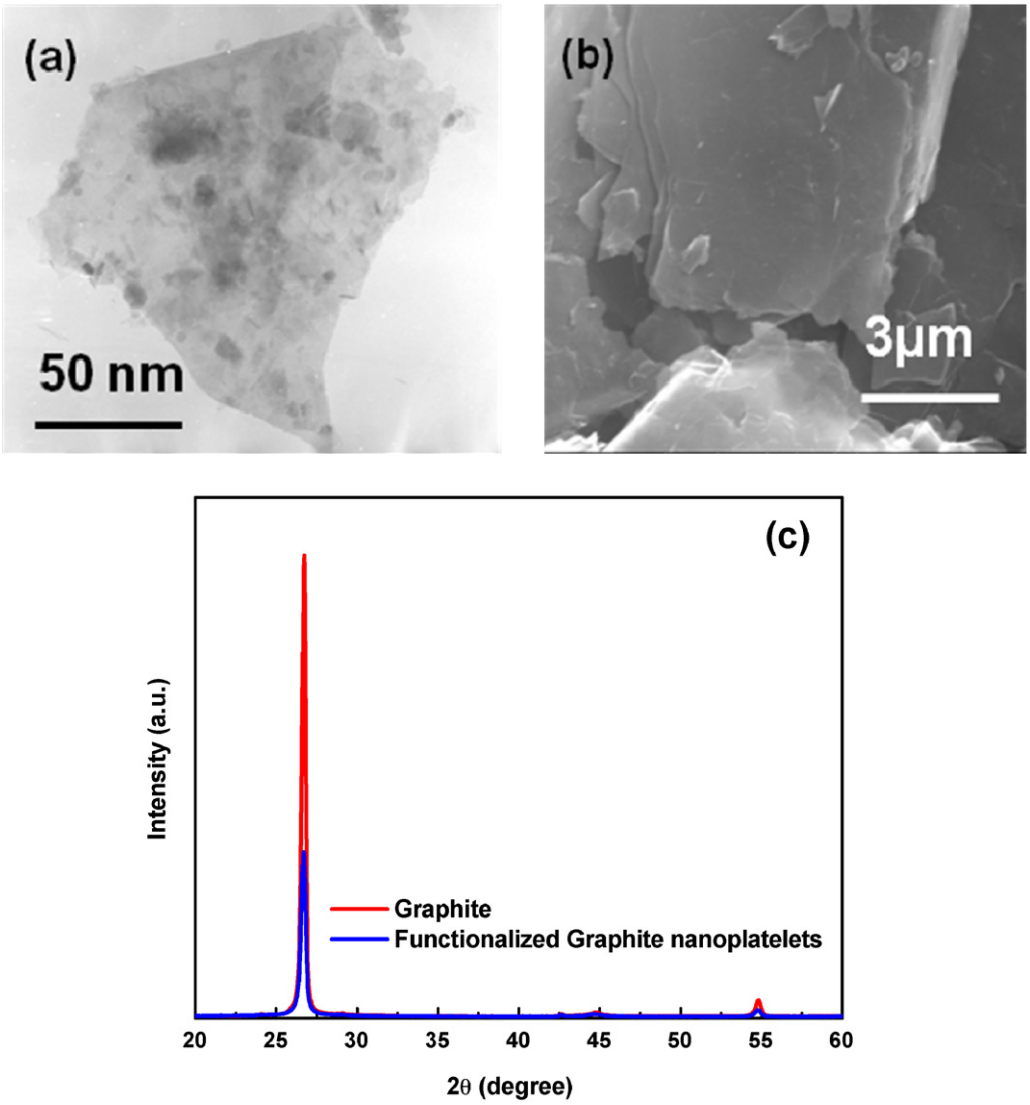

Fig. 2. (a) TEM and (b) SEM images of functionalized graphite nanoplatelets. (c) X-ray diffraction pattern of graphite and functionalized graphite nanoplatelets.

sites on the adsorbents have the same affinity for the adsorbate. Langmuir isotherm is represented by the following equation

$$Q_e = \frac{abC_e}{1 + bC_e} \quad (1)$$

The Freundlich isotherm can be derived from the Langmuir isotherm by assuming that there exists a distribution of sites on the adsorbents for different adsorbates with each site behaving accordingly to the Langmuir isotherm. Freundlich isotherm is represented by the following equation

$$Q_e = k(C_e)^{1/n} \quad (2)$$

where 'Q_e' is the amount of metal impurity adsorbed per unit weight of adsorbent (mg/g), 'C_e' is the equilibrium concentration of water (mg/L), 'b' is the constant related to the free energy of adsorption (L/mg) and 'a' is maximum adsorption capacity. 'k' is the Freundlich constant indicative of the relative adsorption capacity of the adsorbent (mg/g) and ($1/n$) is the adsorption intensity. Q_e is calculated by the following formula

$$Q_e = \frac{(C_0 - C_e)V}{m} \quad (3)$$

where C_0 is the initial concentration of water, 'V' is the volume of water and 'm' is the mass of adsorbent. The isotherms constants for sodium and arsenic with both the isotherms studied were calculated. Fig. 5a shows the comparative fit of Langmuir and Freundlich isotherms with the equilibrium data plotted as Q_e vs. C_e for both arsenic and sodium and isotherm constants values are given in Table 1a. From the experimental results, it can be seen that Langmuir and Freundlich models fit for both metallic impurities (arsenic and sodium). Maximum adsorption capacities for arsenate, arsenite and sodium were found to be nearly 27, 29 and 32 mg/g, respectively. Freundlich constant 'n' was found to be greater than one for both impurities (sodium and arsenic), which is a favorable condition for adsorption [27,28].

3.5. Kinetic studies

The transient behavior of the metal adsorption process was analyzed using Elovich and intra-particle diffusion kinetic models [29–31]. To study the simultaneous transient behavior of sodium and arsenic adsorption, sodium arsenate and sodium arsenite containing aqueous solutions with the initial arsenic concentration of 300 ppm were tested. The linear form of Elovich equation is given

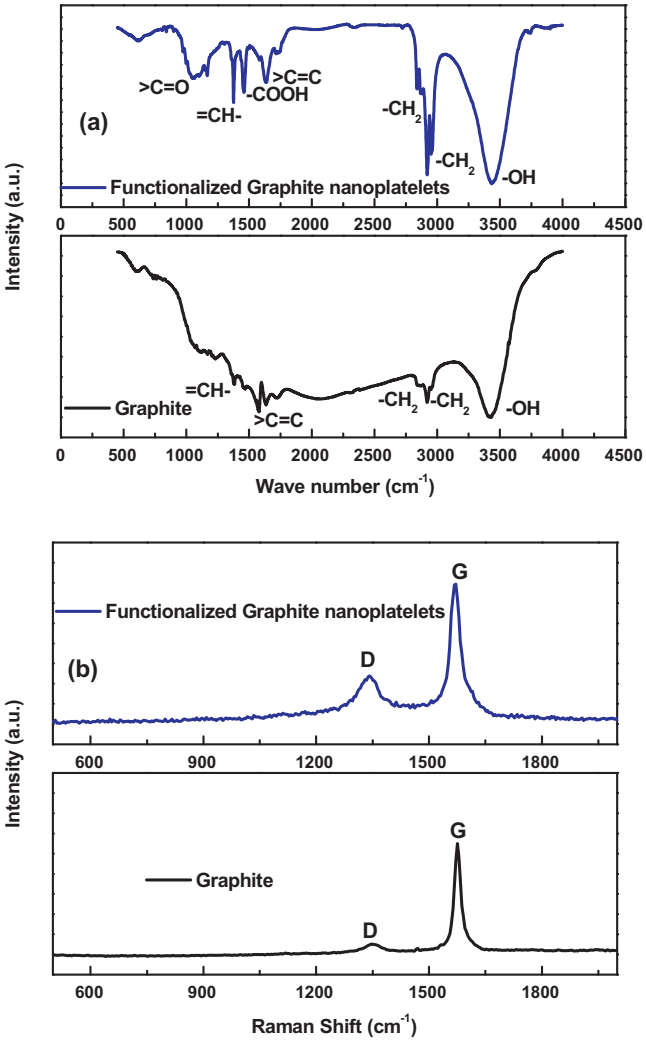

Fig. 3. (a) FTIR spectrum of graphite and functionalized graphite nanoplatelets. (b) Raman spectrum of graphite and functionalized graphite nanoplatelets.

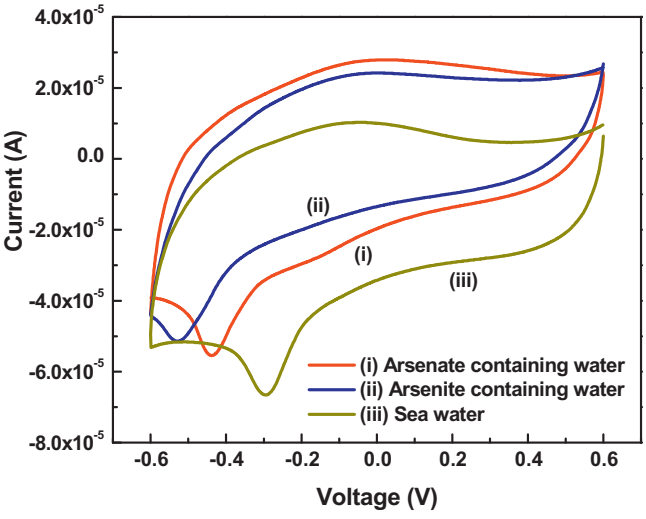

Fig. 4. Cyclic voltamogram of functionalized graphite nanoplatelets for different electrolytes with the scan rate of 10 mV/s.

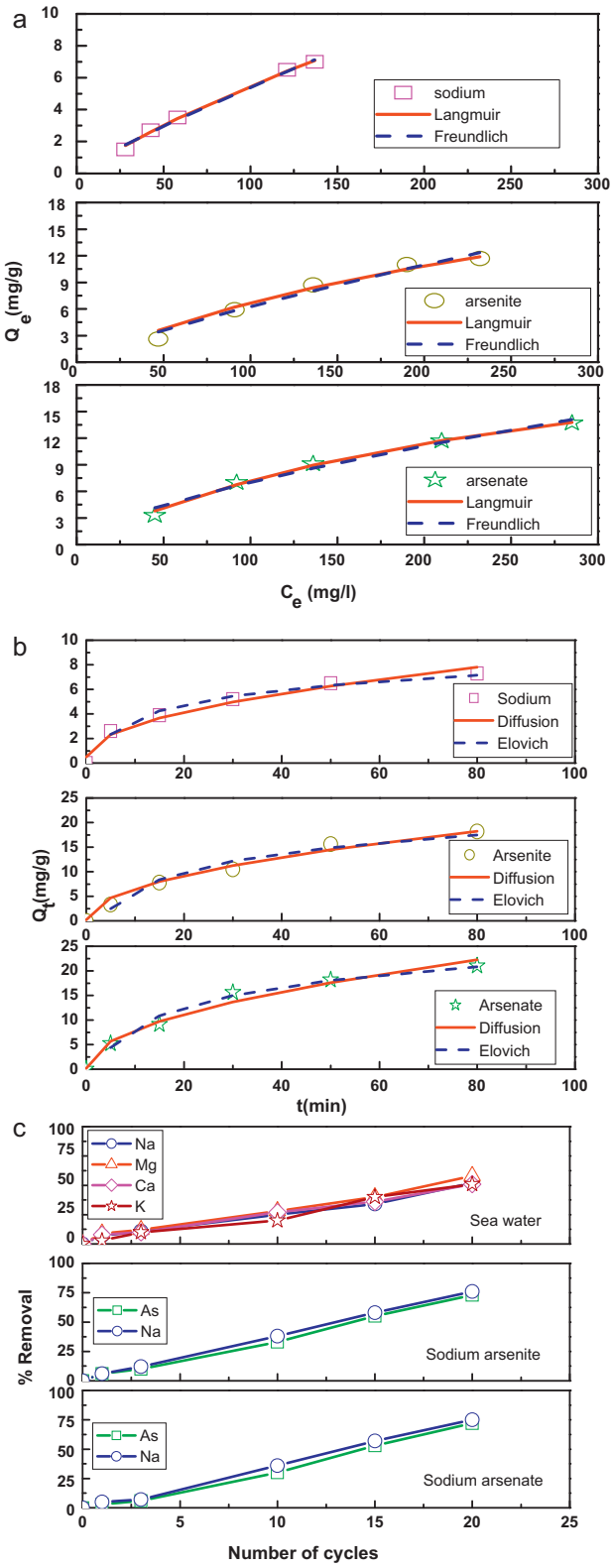

Fig. 5. (a) Isotherm study for sodium and both inorganic arsenic species adsorption. (b) Kinetic study for sodium and both inorganic arsenic species adsorption. (c) Simultaneous removal efficiency for sodium and arsenic with (i) sodium arsenate containing water and (ii) sodium arsenite containing water (iii) removal efficiency for sodium, magnesium, calcium and potassium from sea water.

Table 1
(a) Isotherms constants for arsenic and both inorganic arsenic species adsorption; (b) Kinetics constants for arsenic and both inorganic arsenic species adsorption.

	Sodium	Arsenic (arsenate ion)	Arsenic (arsenite ion)
(a) **Isotherms constants**			
Langmuir			
a (mg/g)	31.98476	27.31206	28.96542
b (L/mg)	0.00208	0.00357	0.003
R^2	0.99592	0.99503	0.97499
Freundlich			
k	0.09868	0.33123	0.15189
n	1.14964	1.50748	1.23808
R^2	0.99383	0.98115	0.96877
(b) **Kinetic constants**			
Elovich			
α (mg/g min)	1.33336	2.47613	1.70607
β (g/mg)	0.5763	0.16847	0.18492
R^2	0.9794	0.9747	0.96625
Intra-particle diffusion			
K (mg/g min$^{1/2}$)	0.8175	2.46979	2.01485
C (mg/g)	0.48926	0.15497	0.2
R^2	0.9796	0.9812	0.98397

by

$$Q_t = \frac{1}{\beta}\ln(\alpha\beta) + \frac{1}{\beta}\ln t \quad (4)$$

The rate constant for intra-particle diffusion (K) is given by

$$Q_t = K(t)^{1/2} + c \quad (5)$$

where 'Q_t' is the amount of metal adsorbed on adsorbent at various time t (mg/g), 'α' is the initial sorption rate (mg/g min), 'β' is the extent of surface coverage (g/mg) and 'K' is the intra-particle diffusion rate constant (mg/g min$^{1/2}$) and c (mg/g) is a constant that gives idea about the thickness of the boundary layer.

The rate constants for sodium and arsenic with both the models were calculated. Fig. 5b shows the comparative fit of Elovich and intra-particle diffusion kinetic models with the equilibrium data plotted as Q_t vs. t for both arsenic and sodium and rate constants values are given in Table 1b. Experimental results suggest that intra-particle diffusion and Elovich models nearly equally fit for both metallic impurities. Elovich model is an adsorption reaction model which originates from chemical reaction kinetics while intra-particle model is a diffusion model. The Elovich curve does not pass through the origin indicates that there is some degree of boundary layer control. However, the intra-particle diffusion curve does not pass through the origin suggesting that intra-particle diffusion model is not the only controlling step. The initial curved portion is attributed to bulk diffusion and the linear portion to intra-particle diffusion [32].

3.6. Removal efficiency

ICP-OES analysis was performed to verify the assumption of CV, which suggests that *f*-GNP are good electrode material for supercapacitor based water filter. ICP-OES analysis gives the actual concentration of metal ions in the solution. % removal efficiency was calculated using the following formula

$$\%\ \text{Removal efficiency} = \frac{(C_0 - C_f)100}{C_0} \quad (6)$$

where 'C_0' is the initial concentration of metal impurity in water and 'C_f' is the final concentration of metal impurity in water after treatment.

To find the cyclic repeatability of the electrode material, different cycles of experiment were performed with high concentration (300 mg/L of As) of arsenic solution and sea water using the same electrode in each cycle. Arsenic solution and sea water was treated for 40 min in each cycle, because the kinetic study clearly shows that after 40 min the adsorption of metal ions (Na and As) approaches to saturation state.

Fig. 5c shows the removal efficiency of supercapacitor based water filter for sodium and both types of arsenic removal and for desalination of sea water. Nearly 72% of arsenic (As) and 75% of sodium (Na) removal efficiency was obtained in case of sodium arsenate containing water, while in the case of sodium arsenite containing water it was found to be 73% and 76% for 'As' and 'Na', respectively, with 20 number of repeated cycles and 100 mg of *f*-GNP loading at each electrode. In each case the initial concentration of arsenic was 300 ppm. Removal of nearly equal % of 'As' and 'Na' in either case suggests the removal of each metallic impurity without getting affected by the other impurities. Almost linear variation in plot suggests the good cyclic repeatability of electrodes for simultaneous removal of arsenic and sodium. Good cyclic repeatability for metal removal performance suggests that *f*-GNP based supercapacitor can be used for the purification of water (sea water) containing high concentrations of multiple metal impurities. Sodium, magnesium, calcium and potassium are found to be most abundant metal impurities in sea water. Therefore removal of Na, Mg, Ca and K from sea water was checked with 100 mg of *f*-GNP at each electrode. Removal efficiency was found to be 52, 58, 51 and 51% for Na, Mg, Ca and K, respectively, with 20 numbers of repeated cycles. Initial concentrations of Na, Mg, Ca and K in sea water were found to be 10,000, 1920, 680 and 570 ppm, respectively. Nearly linear variation of removal efficiency with respect to different numbers of cycles was observed. This suggests the cyclic repeatability and hence reproducibility of electrodes for metal removal from sea water. Reduction of arsenic concentration in sea water could not be measured due to the limitation of ICP-OES at much lower concentration of arsenic.

4. Conclusions

The simultaneous removal of sodium and both inorganic arsenic species (arsenate and arsenite) from aqueous solution as well as for removal of multiple metals from sea water has been demonstrated by carbon fabric supported *f*-GNP electrodes based supercapacitor. Functionalization of GNP provides better contact between electrodes and water, resulting in better performance of metals removal from aqueous solution and sea water. Adsorption isotherms fit to Langmuir and Freundlich models for sodium and arsenic. Adsorption kinetics was found to follow both intra-particle diffusion and Elovich model. High removal efficiency and good cyclic repeatability of electrodes has been demonstrated for both types of arsenic ion containing aqueous solution and sea water. Low cost of GNP compared to other adsorbents like carbon nanotubes provides a platform for the development of cost effective water filter.

Acknowledgements

The authors acknowledge the supports of Office of Alumni Affairs, IITM and DST, India. The authors acknowledge SAIF, IIT Madras for its support in ICP-OES and FTIR analysis. One of the authors (Ashish) is thankful to DST India for providing the financial support.

References

[1] M. Demircioglu, N. Kabay, I. Kurucaovali, E. Ersoz, Demineralization by electrodialysis (ED) – separation performance and cost comparison for monovalent salts, Desalination 153 (2003) 329–333.
[2] M.Y. El-Sayed, Thermoeconomics of some options of large mechanical vapor-compression units, Desalination 125 (1999) 251–257.
[3] A. Grundisch, B. Schneider, Optimising energy consumption in SWRO systems with brine concentrators, Desalination 138 (2001) 223–229.

[4] R. Semiat, Y. Galperin, Effect of non-condensable gases on heat transfer in the tower MED seawater desalination plant, Desalination 140 (2001) 27–46.
[5] R. Semiat, Energy issues in desalination processes, Environ. Sci. Technol. 42 (2008) 8193–8201.
[6] M. Jang, W. Chen, F.S. Cannon, Preloading hydrous ferric oxide into granular activated carbon for arsenic removal, Environ. Sci. Technol. 42 (2008) 3369–3374.
[7] D.L. Boccelli, M.J. Small, D.A. Dzombak, Enhanced coagulation for satisfying the arsenic maximum contaminant level under variable and uncertain conditions, Environ. Sci. Technol. 39 (2005) 6501–6507.
[8] B.K. Mandal, K.T. Suzuki, Arsenic round the world: a review, Talanta 58 (2002) 201–235.
[9] M.M. Benjamin, R.S. Sletten, R.P. Bailey, T. Bennet, Sorption and filtration of metals using iron-oxide-coated sand, Water Res. 30 (1996) 2609–2620.
[10] E.O. Kartinen, C.J. Martin, An overview of arsenic removal processes, Desalination 103 (1995) 79–88.
[11] S. Deng, G. Yu, S. Xie, Q. Yu, J. Huang, Y. Kuwaki, M. Iseki, Enhanced adsorption of arsenate on the aminated fibers: sorption behavior and uptake mechanism, Langmuir 24 (2008) 10961–10967.
[12] J. Zhang, R. Stanforth, Slow adsorption reaction between arsenic species and Goethite (α-FeOOH): diffusion or heterogeneous surface reaction control, Langmuir 21 (2005) 2895–2901.
[13] Y. Wu, X. Ma, M. Feng, M. Liu, Behavior of chromium and arsenic on activated carbon, J. Hazard. Mater. 159 (2008) 380–384.
[14] P. Mondal, C.B. Majumder, B. Mohanty, Treatment of arsenic contaminated water in a batch reactor by using *Ralstonia eutropha MTCC 2487* and granular activated carbon, J. Hazard. Mater. 153 (2008) 588–599.
[15] C. Solisio, M. Panizza, P. Paganelli, G. Cerisola, Electrochemical remediation of copper (II) from an industrial effluent part I: monopolar plate electrodes, Resour. Conserv. Recy. 26 (1999) 115–124.
[16] K. Pruksathorn, H. Vergnes, J. Cantet, P. Duverneuil, Removal of metals in sludge of wastewater treatment, AIDIC Conf. Ser. 4 (1999) 147–152.
[17] A.K. Mishra, S. Ramaprabhu, Magnetite decorated multiwalled carbon nanotubes based supercapacitor for arsenic removal and desalination of sea water, J. Phys. Chem. C 114 (2010) 2583–2590.
[18] S. Ganguli, A.K. Roy, D.P. Anderson, Improved thermal conductivity for chemically functionalized exfoliated graphite/epoxy composites, Carbon 46 (2008) 806–817.
[19] N. Jha, S. Ramaprabhu, Synthesis and thermal conductivity of copper nanoparticle decorated multiwalled carbon nanotubes based nanofluids, J. Phys. Chem. C 112 (2008) 9315–9319.
[20] Y. Geng, S.J. Wang, J.K. Kim, Preparation of graphite nanoplatelets and graphene sheets, J. Colloid Interf. Sci. 336 (2009) 592–598.
[21] U.J. Kim, C.A. Furtado, X. Liu, G. Chen, P.C. Eklund, Raman and IR spectroscopy of chemically processed single walled carbon nanotubes, J. Am. Chem. Soc. 127 (2005) 15437–15445.
[22] A.L.M. Reddy, S. Ramaprabhu, Nanocrystalline metal oxides dispersed multiwalled carbon nanotubes as supercapacitor electrodes, J. Phys. Chem. C 111 (2007) 7727–7734.
[23] Q. Weizhon, T. Liu, F. Wei, Z. Whang, G. Luo, H. Yu, Z. Li, The evaluation of the gross defects of carbon nanotubes in a continuous CVD process, Carbon 41 (2003) 2613–2617.
[24] Z. Wei, P. Somasundaran, Cyclic voltammetric study of arsenic reduction and oxidation in hydrochloric acid using a PtRDE, J. Appl. Electrochem. 34 (2004) 241–244.
[25] I. Langmuir, The adsorption of gases on plane surfaces of glass, mica and platinum, J. Am. Chem. Soc. 40 (1918) 1361–1403.
[26] H.M.F. Freundlich, Over the adsorption in solution, J. Phys. Chem. 57 (1906) 385–471.
[27] Q.U. Jiuhui, Research progress of novel adsorption processes in water purification: a review, J. Environ. Sci. 20 (2008) 1–13.
[28] M. Auffan, J. Rose, O. Proux, D. Borschneck, A. Masion, P. Chaurand, J.L. Hazemann, C. Chaneac, J.P. Jolivet, M.R. Wiesner, A.V. Geen, J.Y. Bottero, Enhanced adsorption of arsenic onto maghemites nanoparticles: as (iii) as a probe of the surface structure and heterogeneity, Langmuir 24 (2008) 3215–3222.
[29] H.A. Taylor, N. Thon, Kinetics of chemisorptions, J. Am. Chem. Soc. 74 (1952) 4169–4173.
[30] M. Ozacar, I.A. Sengil, A kinetic studies of metal complex dye sorption onto pine saw dust, Process Biochem. 40 (2005) 565–572.
[31] H. Qiu, B.C. Pan, Q.J. Zhang, W.M. Zhang, Q.X. Zhang, Critical review in adsorption kinetic models, J. Zhejiang Univ. Sci. A 10 (2009) 716–724.
[32] N. Thinakaran, P. Panneerselvam, P. Baskarlingam, D. Elango, S. Sivanesan, Equilibrium and kinetic studies on the removal of Acid Red 114 from aqueous solutions using activated carbons prepared from seed shells, J. Hazard. Mater. 158 (2008) 142–150.